Broadcasting Brake Lights with MIMO-OFDM Based Vehicular VLC

Bugra Turan[1], Omer Narmanlioglu[2], Sinem Coleri Ergen[1] and Murat Uysal[2]

[1]Department of Electrical and Electronics Engineering, Koc University, Sariyer, Istanbul, Turkey, 34450
E-mail: bturan14@ku.edu.tr, sergen@ku.edu.tr
[2]Department of Electrical and Electronics Engineering, Ozyegin University, Istanbul, Turkey, 34794
E-mail: omer.narmanlioglu@ozyegin.edu.tr, murat.uysal@ozyegin.edu.tr

***Abstract*—Inter-vehicular connectivity to enhance road safety and enable highly autonomous driving is increasingly becoming popular. Despite the prevalent works on radio-frequency (RF) based vehicular communication schemes, visible light communication (VLC) is considered to be a promising candidate for vehicular communications due to its low complexity and RF interference-free nature. This paper investigates applicability of VLC to enhance road safety based on real world measurements. Deployment of multiple light emitting diodes (LEDs) enables multiple-input multiple-output (MIMO) transmission in the context of vehicular VLC. We consider direct current biased optical orthogonal frequency division multiplexing (DCO-OFDM) based MIMO transmission scheme and evaluate the performances of different MIMO modes including repetition code (RC) and spatial multiplexing (SM), different modulation orders and different transmitter-receiver selection. The results reveal that selection of the closest transmitters to the receivers, provide better performance due to high signal-to-noise-ratio (SNR) requirements for RC mode. However, usage of all possible transmitters does not always yield better performance due to power division at the transmitter side. Moreover, SM suffers from channel correlation whereas the performance of RC shows more degradation on higher-order modulations that are required to yield the same throughput with SM.**

***Index Terms*—Vehicular communication, visible light communication, MIMO, OFDM.**

I. Introduction

Increasing road safety and enabling autonomous driving are considered within the ultimate goals of the future of mobility. Environmental perception based on Advanced Driver Assistance Systems (ADAS) such as automotive radar, lidar, cameras and ultrasonic sensors are believed to be key for realizing highly automated driving. Moreover, vehicle to everything (V2X) connectivity schemes such as Long Term Evolution (LTE) and Dedicated Short Range Communication (DSRC) aim to increase situational awareness, providing non-line-of-sight (NLoS) road and traffic information. LTE, offering wide coverage and supporting different communication types is expected to fulfill the quality-of-service (QoS) requirements of V2X services [1]. On the other hand, DSRC, offering decentralized and infrastructure-less framework with low latency is another candidate for vehicle to vehicle communications (V2V). Hybrid vehicular communication architectures are also proposed to take full advantage of the LTE and DSRC in dense traffic scenarios. It is shown that hybrid V2V architectures provide less end-to-end delay as contention probability is decreased [2].

V2V is foreseen to play major role for road safety with the emerging autonomous driving features on manually driven vehicles and the prospective fully autonomous vehicles. V2V aims to extend perception range of on board ADAS sensors, enabling cooperative sensing. Furthermore, V2V, conveying acceleration, deceleration, wheel slip and road surface condition information, is provisioned to increase traffic flow and smoothness, reducing fluctuations sourced by speed variations with the deployment of cooperative adaptive cruise control [3].

However, with the autonomous driving, small inter-vehicle distances with high density of traffic is likely to cause higher data load and increase end-to-end delay in the network. Even though LTE is foreseen to meet latency requirements from 20 msec for pre-crash sensing to 100 msec for other applications [4], lack of infrastructure support and lower latency requirements less than 5 msec proposed by METIS [5] brings the question about the adoption of LTE for V2V. Moreover, radio frequency (RF)-based DSRC [6] and LTE [7] are prone to intentional jamming and malicious attacks, which may result in communication delays, disruptions or throughput degradations. Thus, additional communication standards are needed to fulfill stringent autonomous driving requirements, as current vehicular connectivity schemes do not target autonomous driving [8], in terms of network off-loading, better spectrum usage and enhanced security.

In addition to RF based LTE and DSRC, visible light communication (VLC) [9] is regarded as a low cost complementary solution to off-load network, providing line-of-sight (LoS), RF interference free and secure communication medium. VLC, uses optical radiation of modulated light emitting diodes (LEDs) at the visible light spectrum between 390 THz and 700 THz. LEDs providing optical modulation frequencies up to a few hundred MHz [10] at the transmitter with the high bandwidth photodetectors (PDs) at the receiver side are promising $\mathrm{Gbit/s}$ data rates for VLC. Moreover, cameras and solar cells are also envisaged to be employed as communication receivers for VLC [11].

Recently, vehicles started to be equipped with LED lights. Compared to halogen and high intensity discharge bulbs, LED counterparts offer longer life time, better illumination and

978-1-5090-5197-7/16/$31.00 ©2016 IEEE

energy savings. Furthermore, LEDs are shown to be utilized for LoS vehicular communications. In [12], authors summarize the vehicular VLC experimental studies and investigate VLC only, DSRC only and VLC/DSRC Hybrid usage scenarios in simulation environment. [13] evaluates 2x2 optical multiple input multiple output (MIMO) VLC with LED headlights. [14] takes into account the actual LED headlight radiation pattern to evaluate vehicular VLC performance as commonly used single LED Lambertian radiation pattern is not applicable to automotive lights. Moreover, [15] highlights the security aspects of VLC usage for vehicular communications, proposing a hybrid architecture including DSRC under simulations.

Several optical MIMO techniques [16]–[20] and modulation schemes have been studied to provide robust, high rate communications using LEDs with limited modulation bandwidths. [16] proposes optical space modulation techniques using Lambertian radiation pattern of LEDs for MIMO schemes comparison while [17]–[19] studies MIMO techniques for indoor usage scenarios. Optical MIMO is also proposed to replace physical transmitter-receiver alignment requirements for LoS VLC by electronic alignment [21]. To best of our knowledge, none of the studies to date, considered various optical MIMO and modulation scheme selections, based on the measured automotive LED radiation pattern.

In this paper, we propose performance comparison of optical MIMO and modulation selection schemes, based on the measured channel model of vehicle brake lights with varying vehicle locations. The novel contributions of this study are threefold. First, measuring the received optical power from LED brake lights of a production vehicle, we obtained the realistic channel model. Then, we evaluate the selection of the best LED transmitter configuration for repetition coding (RC) and spatial multiplexing (SM) MIMO schemes depending on the obtained channel model. Finally, we provide performance comparison between different MIMO schemes including RC and SM and modulation orders with respect to the following vehicle's locations.

The rest of this paper is organized as follows. Section II describes the system model including utilized optical MIMO transmission and related bit-error-rate (BER) expressions. Section III, presents the considered inter-vehicular VLC experimental setup with measured channel model. Section IV provides the performance evaluation of the selected system structures. Finally, we conclude the paper in Section V.

Notation: $||.||^2$, $(.)^*$ and $[.]^{\mathrm{T}}$ denote Euclidean distance, complex conjugate and transpose, respectively. $Q(.)$ is the tail probability of standard normal distribution.

II. System Model

In the system model, we consider optical LoS MIMO transmission schemes with N_T transmitter LEDs and N_R receiver PDs. LEDs are assumed to be concurrently driven by the same hardware. Path differences between various transmitter-receiver links are considered to be compensated. Moreover, perfect synchronization with the transmitters is presumed.

Orthogonal frequency-division multiplexing (OFDM) in intensity modulation and direct detection (IM/DD) optical wireless communications is known for its ability to compensate signal dispersion, when compared to conventional pulse position modulation (PPM) and on-off keying (OOK) modulation schemes. Optical OFDM, requires real valued and non-negative signals to be transmitted. Hence, DC bias addition is used to drive the LEDs for direct current biased optical orthogonal frequency-division multiplexing (DCO-OFDM) [22], while clipping signals at zero and transmitting solely the positive parts is considered with asymmetrically-clipped optical OFDM (ACO-OFDM). DCO-OFDM is known to be more bandwidth efficient than ACO-OFDM and its performance depends on the bias level. Regarding automotive lighting with certain required bias level, to take advantage of the bandwidth efficiency, we select DCO-OFDM to modulate the information bits. The block diagram of single-input single-output (SISO) DCO-OFDM transmission is given in Fig. 1.

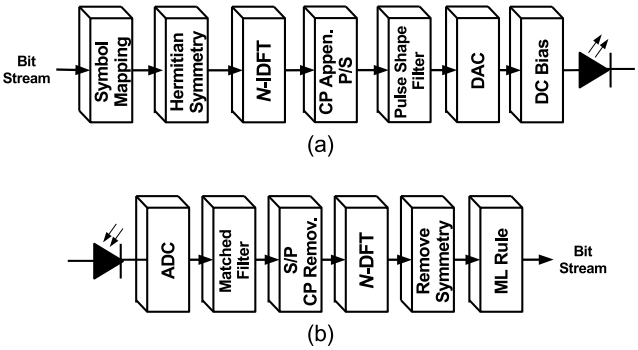

Figure 1: Block diagram of DCO-OFDM (a) transmitter and (b) receiver.

It is known that the inverse discrete Fourier transform (IDFT) response of complex or real valued vector satisfying Hermitian symmetry becomes real. When the DCO-OFDM frame size without cyclic prefix (CP) is set to N, symbols (s) generated responding to $M-$ary phase-shift keying (PSK) or quadrature amplitude modulation (QAM), are re-arranged with respect to Hermitian symmetry such as,

$$\mathbf{X} = [0 \; s_1 \; s_2 \; s_3 \; ... \; s_{N/2-1} \; 0 \; s^*_{N/2-1} \; ... \; s^*_2 \; s^*_1]^{\mathrm{T}}, \quad (1)$$

before IDFT process, hence, the output becomes real valued. After CP appending with the length of N_{CP}, DC bias (V_{bias}) is added to shift the signal into the linear operation range of the LEDs, limited by turn-on voltage (V_{tov}) and maximum-allowed voltage (V_{max}). Signals beyond this range will be clipped, therefore, the signal power level is set corresponding to the linear operation range of LEDs.

The frequency-domain received signal at the n^{th} PD with N_T transmitter LEDs can be written as

$$Y_n[k] = \sum_{m=1}^{N_T} \sqrt{\frac{P}{N_T}} R X_m[k] h_{nm} + V_n[k] \quad (2)$$

where P is the total electrical OFDM signal power, R is the optical-to-electrical conversion coefficient (A/W) of PD, h_{nm} is the frequency response of optical communication channel between n^{th} PD and m^{th} LED and $V_n[k]$ is additive white Gaussian noise (AWGN) with zero mean and σ_N^2 variance calculated by $N_0 W$ where N_0 is power spectral density and W is system bandwidth at n^{th} PD. RC and SM optical MIMO schemes are considered to evaluate the performance of the proposed experimental setup.

A. Repetition Coding MIMO

In RC, same information is transmitted by each LED simultaneously, resulting intensities to constructively add up at the receiver. DCO-OFDM achieves a spectral efficiency of $(\log_2 M)/2$ bit/s/Hz (assume N is large enough) where M is the modulation order. *Maximum Likelihood* (ML) decision rule can be written as,

$$\hat{X}[k] = \underset{X \in \Omega}{\operatorname{argmin}} \left(\sum_{n=1}^{N_R} \left\| \frac{Y_n[k]}{\sqrt{\frac{P}{N_T}} R} - X \sum_{m=1}^{N_T} h_{nm} \right\|^2 \right) \tag{3}$$

where Ω is the set of constellation points of deployed modulation scheme and signal-to-noise ratio (SNR) per subcarrier is,

$$\mathrm{SNR}[k] = \frac{\frac{PR^2}{N_T} \sum_{n=1}^{N_R} \left| \left(\sum_{m=1}^{N_T} h_{nm} \right) \right|^2}{\sigma_N^2}. \tag{4}$$

Moreover, subcarrier-based BER can be calculated by (7) [23].

B. Spatial Multiplexing MIMO

In SM, each LED disseminates different information at the same time. SM with DCO-OFDM offers enhanced spectral efficiency of $(\min(N_T, N_R) \log_2 M)/2$ bit/s/Hz. ML decision rule is given by,

$$\hat{\mathbf{X}}[k] = \underset{\mathbf{X} \in \mathbf{\Phi}}{\operatorname{argmin}} \left(\left\| \mathbf{Y}[k] - \sqrt{\frac{P}{N_T}} R \mathbf{H} \mathbf{X} \right\|^2 \right) \tag{5}$$

where $\mathbf{Y}[k]$ is the received signal vector with the dimension of N_R, $\mathbf{H}$ is $N_R \mathrm{x} N_T$ channel matrix on the k^{th} subcarrier and Φ includes all possible combinations of transmitted signal vectors. The upper bound of subcarrier based BER values given by ML decision rule can be calculated by (8) (see the top of the next page) where $\mathrm{d_H}(\mathbf{b_{m_1}}, \mathbf{b_{m_2}})$ is Hamming distance of two bit assignments, which are $\mathbf{b_{m_1}}$ and $\mathbf{b_{m_2}}$, of the signal vectors $\mathbf{s_{m_1}}$ and $\mathbf{s_{m_2}}$ [17]. The overall BER in DCO-OFDM can be calculated by

$$\mathrm{BER} = \frac{2}{N-2} \sum_{k=1}^{N/2-1} \mathrm{BER_{RC,SM}[k]} \tag{6}$$

III. Experimental Setup

Night time driving on a three lane road is considered in the experimental setup. Leading vehicle, equipped with three LED brake lights, is assumed to be transmitting information solely with its brake lights. Night time optical received power measurements are conducted up to 20 m for three different lanes. Leading vehicle is positioned in the middle lane, while the following vehicles are assumed to be proceeding in all three lanes (i.e L1, L2, L3) as depicted on Fig. 3. Single vehicle with two receivers is considered to be at 30 different direct LoS positions for each measurement (i.e. 3 lanes at every 2 m up to 20 m). Thereby, communication possibility with respect to received optical power is inspected for various receiver angles and distances. Moreover, both leading and following vehicles are assumed to be proceeding on a straight three lane road as additional challenges such as blocking and power imbalance on curvy roads are beyond the scope of this paper.

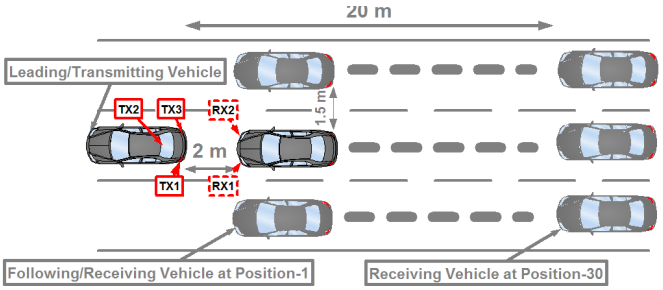

Figure 2: Measurement scenario.

No modifications were made on the leading vehicle's brake lights to measure their radiation pattern. It is worth to note that, each brake light is made up of an array of LEDs. Left and right brake lights are encapsulated under taillight housing with optical reflector and concentrators. Hence, Lambertian radiation pattern is not applicable to the brake lights under interest. On the contrary to headlights, taillights have symmetrical illumination pattern, consistent with the regulation [24], as depicted on Fig. 4 (a)-(b). Third brake light (see Fig. 3−Tx2) is made up from an array of 8 LEDs located at the top of the rear windshield. Taillights separation distance is 70 cm, while the third brake light is 1 m away from each taillight's inner corner. Left and right brake lights transmit optical power of 10 dBm whereas the third brake light emits −8 dBm of optical power.

Figure 3: Experimental setup.

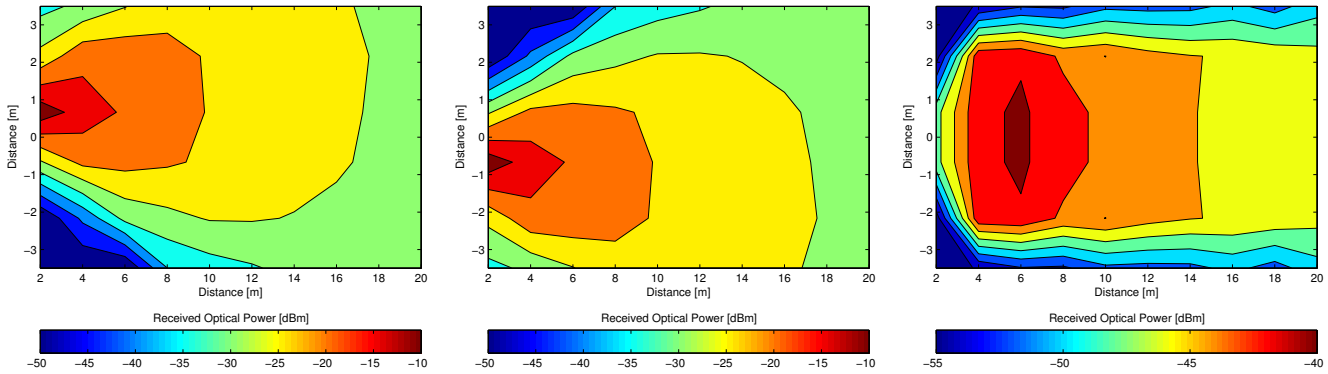

(a) (b) (c)

Figure 4: (a) Right LED Brake Light (b) Left LED Brake Light (c) Third LED Brake Light.

$$\mathrm{BER}_{\mathrm{RC}}[k] \approx \begin{cases} Q\left(\sqrt{2\mathrm{SNR}[k]}\right) & , \quad 2-\mathrm{PSK} \\ \frac{2\left(\sqrt{M}-1\right)}{\sqrt{M}\log_2\sqrt{M}} Q\left(\sqrt{\frac{3\mathrm{SNR}[k]}{(M-1)}}\right) & , \quad \mathrm{square}-M-\mathrm{QAM} \\ \frac{2}{\log_2(U\mathrm{x}J)}\left[\frac{U-1}{U} Q\left(\sqrt{\frac{6\mathrm{SNR}[k]}{U^2+J^2-2}}\right) + \frac{J-1}{J} Q\left(\sqrt{\frac{6\mathrm{SNR}[k]}{U^2+J^2-2}}\right)\right] & , \quad \mathrm{rectangular}-M=U\mathrm{x}J-\mathrm{QAM} \end{cases} \tag{7}$$

$$\mathrm{BER}_{\mathrm{SM}}[k] \leq \frac{1}{M^{N_T}\log_2\left(M^{N_T}\right)} \sum_{m_1=1}^{M^{N_T}} \left(\sum_{m_2=1}^{M^{N_T}} \mathrm{d_H}\left(\mathbf{b_{m_1}}, \mathbf{b_{m_2}}\right) Q\left(\sqrt{\frac{PR^2}{2\sigma_N^2 N_T}\left\|\mathbf{H}[k]\left(\mathbf{s_{m_1}}-\mathbf{s_{m_1}}\right)\right\|^2}\right)\right) \tag{8}$$

Received power is measured using Thorlabs PM 200 optical power meter with S142C PD and FGL610 Colored Glass Filter in order to avoid artificial light interference below 610 nm wavelength. Each following vehicle is assumed to be equipped with two receivers at the height of 80 cm, adjacent to the left and right headlights with a separation distance of 1.33 cm. Vehicles in nearby lanes are considered to be 1.5 m separated from each other. Test field is selected to be free of additional road side objects, for the purpose of preventing reflection effects on the received optical power. Received optical power measurements are conducted separately for each brake light. Radiation from single light source is measured while the other two lights were blocked. Thereby, measurement results are utilized to evaluate the performances of various MIMO configurations detailed in Section II.

Table I: Transmission modes.

Mode	Modulation	MIMO Type	Configuration
1	4−QAM (16−QAM)	RC	C1
2	4−QAM (16−QAM)	RC	C2
3	4−QAM (16−QAM)	RC	C3
4	4−QAM (16−QAM)	RC	C4
5	2−PSK (4−QAM)	SM	C1
6	2−PSK (4−QAM)	SM	C2
7	2−PSK (4−QAM)	SM	C3

Table II: Simulation Parameters.

LED modulation bandwidth (W)	20 MHz
Power spectral density of VLC noise (N_0)	10^{-22} W/Hz
Responsivity of PD (R)	1.0 A/W
Number of subcarrier (N)	64
Length of cyclic prefix (N_{CP})	4

IV. Numerical Results

In this section, performance evaluation of seven different transmission modes summarized in Table I is conducted and the best scheme with respect to vehicle locations is provided. We consider four different transmitter with fixed dual receiver configurations, namely C1, C2, C3 and C4. C1 transmitter configuration denotes the usage of left and right brake lights, C2 utilizes left and third brake lights while C3 employs right and third brake light whereas C4 configuration uses all three brake lights. Dual receiver configuration indicates the PDs located near the left and right headlight of the following vehicle. Hence, four different MIMO configurations are studied, including three 2x2 and one 3x2 MIMO setups. The performance of RC MIMO mode is investigated with all four configurations whereas only the 2x2 MIMO configurations are considered for SM MIMO mode. We consider another two cases which have different spectral efficiencies. In order to yield equal throughput, for 2−PSK modulation scheme in

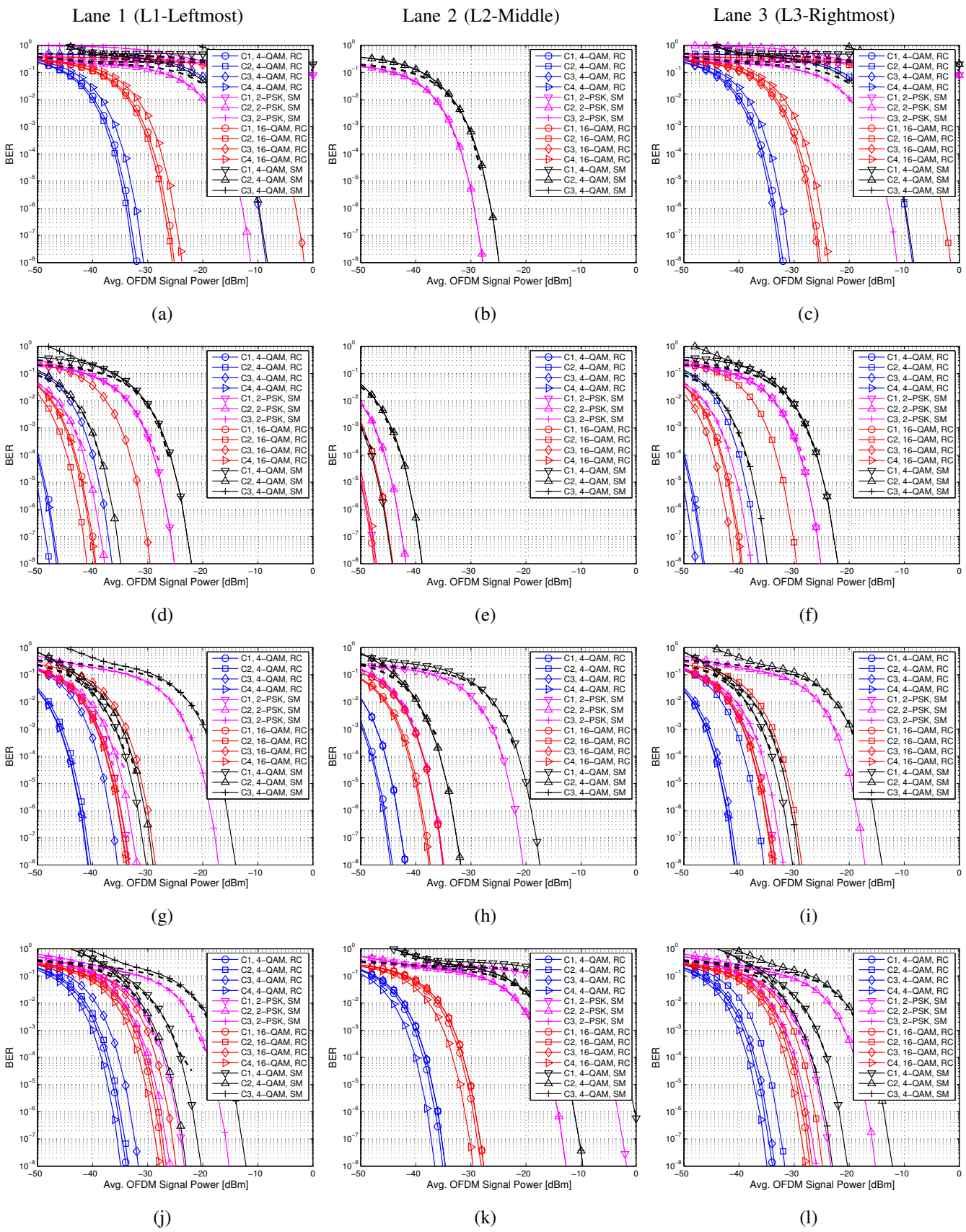

Figure 5: BER performances on different lanes with the distances of (a,b,c) 2 m, (d,e,f) 6 m, (g,h,i) 12 m and (j,k,l) 20 m.

Table III: The minimum required average DCO-OFDM signal power levels in dBm to achieve target BER of 10^{-6}.

		Lane 1				Lane 2				Lane 3			
		2 m	6 m	12 m	20 m	2 m	6 m	12 m	20 m	2 m	6 m	12 m	20 m
4-QAM RC	C1	-33.16	-47.39	-42.03	-35.13	**-69.72**	**-55.65**	-45.34	-36.18	-33.16	-47.39	-42.03	-35.13
	C2	**-33.61**	**-49.09**	-41.43	-34.75	-66.59	-52.21	-43.11	-35.93	-9.699	-37.61	-36.66	-33.02
	C3	-9.699	-37.61	-36.66	-33.02	-66.59	-52.21	-43.11	-35.93	**-33.61**	**-49.09**	-41.43	-34.75
	C4	-32.02	-47.82	**-42.06**	**-36.08**	-68.05	-55.15	**-45.78**	**-37.74**	-32.02	-47.82	**-42.06**	**-36.08**
2-PSK SM	C1	13.53	-26.28	-34.48	-24.53	-69.51	-48.51	-21.85	-3.075	13.53	-26.28	-34.48	-24.53
	C2	-12.46	-39.11	-33.20	-27.20	-29.11	-43.10	-36.12	-14.04	13.53	-26.28	-18.27	-16.36
	C3	13.53	-26.28	-18.27	-16.36	-29.11	-43.10	-36.12	-14.04	-12.46	-39.11	-33.20	-27.20
16-QAM RC	C1	-26.25	-40.56	-35.07	-28.21	-63.01	**-48.91**	-38.49	-29.28	-26.25	-40.56	-35.07	-28.21
	C2	**-26.86**	**-42.15**	-34.61	-28.00	-59.83	-45.31	-36.18	-29.02	-2.978	-30.86	-29.93	-26.07
	C3	-2.978	-30.86	-29.93	-26.07	-59.83	-45.31	-36.18	-29.02	**-26.86**	**-42.15**	-34.61	-28.00
	C4	-25.06	-41.01	**-35.12**	**-29.14**	-61.10	-48.23	**-39.00**	**-31.00**	-25.06	-41.01	**-35.12**	**-29.14**
4-QAM SM	C1	16.54	-23.27	-31.46	-21.51	**-66.50**	-45.50	-18.83	-0.071	16.54	-23.27	-31.46	-21.51
	C2	-9.454	-36.11	-30.19	-24.20	-26.11	-40.09	-33.11	-11.04	16.54	-23.27	-15.26	-13.35
	C3	16.54	-23.27	-15.26	-13.35	-26.11	-40.09	-33.11	-11.04	-9.454	-36.11	-30.19	-24.20

SM, $4-$QAM is selected in RC. Similarly, when $4-$QAM is selected for SM, RC with $16-$QAM is considered in transmission modes.

We present numerical results to evaluate the BER performance of transmission modes at different lanes and distances. The simulation parameters are given in Table II. During simulations, we assumed that the perfect channel state information (CSI) is available at the receiver unit.

In Fig. 5, the BER performances of considered transmission modes are presented at different lanes and distances with respect to the different average signal power levels. Monte Carlo simulation results are also shown by dashed lines whereas the theoretical results are shown by solid lines with different markers. In high SNR region, perfect match with theoretical results are obtained for both RC and SM modes. Based on these figures (with the extension of signal power range), the minimum required average DCO-OFDM signal power levels (in dBm) that satisfies the target BER of 10^{-6} are listed in Table III. For each case (RC with $4-$QAM/SM with $2-$PSK and RC with $16-$QAM/SM with $4-$QAM), the best transmitter selection and MIMO mode with corresponding modulation order is emphasized with bold. Lower minimum required average DCO-OFDM signal power levels denotes the better channel gain for the selected modulation order and MIMO scheme. Therefore, selecting the minimum signal power level for each distance within the considered scheme, best transmitter configurations are obtained. Moreover, $4-$QAM with $2-$PSK SM and $16-$QAM RC with $4-$QAM SM are evaluated together, as they are intended to provide the same throughput.

In Table III and Fig. 5, it is observed that RC with the usage of left and third brake lights (C2) outperforms the rest in lane 1 with the distance of 2 m and 6 m. This situation is valid for both cases that give different throughput. For lane 1 with the distances of 12 m and 20 m, RC with $\mathrm{C4}$ configuration satisfies the target BER of 10^{-6} with the lowest average transmitted power level. Whenever lane 2 with the distance of 2 m is considered, RC with right and left brake lights ($\mathrm{C1}$) gives the highest performance for first case, however, SM with $4-$QAM using the same configuration outperforms RC with $16-$QAM with the gain of approximately 3 dB. At the distance of 6 m, RC with the same configuration gives the best performance, however, inspecting distances of 12 m and 20 m, usage of all brake lights ($\mathrm{C4}$) increases the SNR level at the receiver side. For lane 3, similar to lane 1, RC outperforms SM at the distance of 2 m, 6 m, 12 m and 20 m, while the best configurations are with the usage of right and third brake lights ($\mathrm{C3}$) for the first two distances and using all brake lights ($\mathrm{C4}$) for the last two distances of interest. Furthermore, it is observed that with the increasing modulation order at the lane 2 for 2 m distance, RC shows degraded performance when compared to SM. At 2 m distance, each brake light is conceived more like a point source instead of diffuse source, resulting with less channel correlation, favorable for SM. However, RC requires more increase in the SNR for higher modulation orders, as it lacks multiplexing gain.

In Fig. 5 it can also be observed that, BER performances evaluated for left and right lanes are similar due to the symmetrical radiation patterns of the left and right brake lights, while the third brake light has identical effect for both lanes. Moreover, same BER performances are obtained for $\mathrm{C2}$ and $\mathrm{C3}$ transmitter configurations on the middle lane. As a result of smaller incidence angles when compared to left and right lanes, increased received power is measured for the middle lane. Thereby, lower BER values are attained with respect to the average OFDM signal power levels as depicted on Fig. 5 (b)-(e)-(h)-(k).

It can be concluded that at the distances of 2 m and 6 m $\mathrm{C2}$ and $\mathrm{C3}$ gives the best performances for Lane 1 and Lane 3, respectively, whereas $\mathrm{C1}$ is the best for Lane 2. However, for the distances of 12 m and 20 m, $\mathrm{C4}$ gives the highest performance for all lanes. The results reveal that using all transmitters does not always improve the system performance since it requires transmit power division between transmitters. Utilization of closer transmitters improves the system performance due to the fact that they provide lower path attenuation. Moreover, it can be noticed that SM suffers from channel correlation whereas RC suffers from higher modulation order, however, it is more robust the correlation.

V. Conclusion

In this paper, configuration selection of the optical transmitters and MIMO modes with the corresponding modulation orders are addressed for vehicular VLC with the usage of measured vehicular visible light channel model. Employing the automotive brake lights compliant with the regulation, night time measurements are conducted at practical receiver locations to evaluate the sun light interference free characteristics of optical signals from brake lights. Considering the LoS nature of vehicular VLC channel, use cases such as pre-crash sensing and emergency stop are targeted. We evaluated the system performance in terms of BER and provided a comparison between various MIMO configuration schemes. Our results indicate that nearby transmitters to the receiver are more favorable due to high SNR requirement, however, usage of all possible transmitters does not yield better performance due to power division at the transmitter side. Moreover, SM suffers from channel correlation and it requires high SNR values in low spectral efficiency cases, whereas, RC suffers from higher modulation orders that are required to achieve the same spectral efficiency with SM.

References

[1] H. Seo, K.-D. Lee, S. Yasukawa, Y. Peng, and P. Sartori, "LTE evolution for vehicle-to-everything services," *IEEE Communications Magazine*, vol. 54, no. 6, pp. 22–28, 2016.

[2] K. Katsaros, M. Dianati, R. Tafazolli, and G. Xiaolong, "End-to-End Delay Bound Analysis for Location-based Routing in Hybrid Vehicular Networks," *IEEE Transactions on Vehicular Technology*, vol. PP, no. 99, pp. 1–1, 2015.

[3] W. J. Schakel, B. van Arem, and B. D. Netten, "Effects of cooperative adaptive cruise control on traffic flow stability," in *Intelligent Transportation Systems (ITSC), 2010 13th International IEEE Conference on*, pp. 759–764, IEEE, 2010.

[4] S.-h. Sun, J.-l. Hu, Y. Peng, X.-m. Pan, L. Zhao, and J.-y. Fang, "Support for vehicle-to-everything services based on LTE," *IEEE Wireless Communications*, vol. 23, no. 3, pp. 4–8, 2016.

[5] M. ICT, "317669-METIS/D1., Scenarios, requirements and KPIs for 5G mobile and wireless system," 2013.

[6] S. . Tengstrand, K. Fors, P. Stenumgaard, and K. Wiklundh, "Jamming and interference vulnerability of IEEE 802.11p," in *2014 International Symposium on Electromagnetic Compatibility*, pp. 533–538, Sept 2014.

[7] Y. O. Basciftci, F. Chen, J. Weston, R. Burton, and C. E. Koksal, "How Vulnerable Is Vehicular Communication to Physical Layer Jamming Attacks?," in *Vehicular Technology Conference (VTC Fall), 2015 IEEE 82nd*, pp. 1–5, Sept 2015.

[8] L. Hobert, A. Festag, I. Llatser, L. Altomare, F. Visintainer, and A. Kovacs, "Enhancements of V2X communication in support of cooperative autonomous driving," *IEEE Communications Magazine*, vol. 53, no. 12, pp. 64–70, 2015.

[9] S. Arnon, J. Barry, and G. Karagiannidis, *Advanced optical wireless communication systems*. Cambridge university press, 2012.

[10] I. Dursun, C. Shen, M. R. Parida, J. Pan, S. P. Sarmah, D. Priante, N. Alyami, J. Liu, M. I. Saidaminov, M. S. Alias, *et al.*, "Perovskite Nanocrystals as a Color Converter for Visible Light Communication," *ACS Photonics*, 2016.

[11] Y. Liu, H.-Y. Chen, K. Liang, C.-W. Hsu, C.-W. Chow, and C.-H. Yeh, "Visible light communication using receivers of camera image sensor and solar cell," *IEEE Photonics Journal*, vol. 8, no. 1, pp. 1–7, 2016.

[12] A. Bazzi, B. M. Masini, A. Zanella, and A. Calisti, "Visible light communications as a complementary technology for the internet of vehicles," *Computer Communications*, 2016.

[13] P. Luo, Z. Ghassemlooy, H. Le Minh, E. Bentley, A. Burton, and X. Tang, "Bit-Error-Rate Performance Of a Car-to-Car VLC Ssystem Using 2×2 MIMO," 2015.

[14] M. Uysal, Z. Ghassemlooy, A. Bekkali, A. Kadri, and H. Menouar, "Visible Light Communication for Vehicular Networking: Performance Study of a V2V System Using a Measured Headlamp Beam Pattern Model," *IEEE Vehicular Technology Magazine*, vol. 10, pp. 45–53, Dec 2015.

[15] S. Ishihara, R. V. Rabsatt, and M. Gerla, "Improving reliability of platooning control messages using radio and visible light hybrid communication," in *Vehicular Networking Conference (VNC), 2015 IEEE*, pp. 96–103, Dec 2015.

[16] A. Stavridis and H. Haas, "Performance evaluation of space modulation techniques in VLC systems," in *2015 IEEE International Conference on Communication Workshop (ICCW)*, pp. 1356–1361, June 2015.

[17] T. Fath and H. Haas, "Performance comparison of MIMO techniques for optical wireless communications in indoor environments," *Communications, IEEE Transactions on*, vol. 61, no. 2, pp. 733–742, 2013.

[18] Y. Hong, T. Wu, and L. K. Chen, "On the Performance of Adaptive MIMO-OFDM Indoor Visible Light Communications," *IEEE Photonics Technology Letters*, vol. 28, pp. 907–910, April 2016.

[19] P. F. Mmbaga, J. Thompson, and H. Haas, "Performance Analysis of Indoor Diffuse VLC MIMO Channels Using Angular Diversity Detectors," *Journal of Lightwave Technology*, vol. 34, pp. 1254–1266, Feb 2016.

[20] M. O. Damen, O. Narmanlioglu, and M. Uysal, "Comparative performance evaluation of MIMO visible light communication systems," in *2016 24th Signal Processing and Communication Application Conference (SIU)*, pp. 525–528, IEEE, 2016.

[21] L. Zeng, D. C. O'Brien, H. L. Minh, G. E. Faulkner, K. Lee, D. Jung, Y. Oh, and E. T. Won, "High data rate multiple input multiple output (MIMO) optical wireless communications using white led lighting," *IEEE Journal on Selected Areas in Communications*, vol. 27, pp. 1654–1662, December 2009.

[22] J. Armstrong, "OFDM for optical communications," *Lightwave Technology, Journal of*, vol. 27, no. 3, pp. 189–204, 2009.

[23] K. Cho and D. Yoon, "On the general BER expression of one-and two-dimensional amplitude modulations," *Communications, IEEE Transactions on*, vol. 50, no. 7, pp. 1074–1080, 2002.

[24] "ECE Regulation No. 48, Uniform provisions concerning the approval of vehicles with regard to the installation of lighting and light-signaling devices ," vol. Rev.1/Add.47/Rev.6, pp. 52–54.